2003 Pacific Conference on Earthquake Engineering

Impact of decentralized semi-active control on the stability of tall structures under seismic loading

J. Geoffrey Chase & Stephen Hunt

Department of Mechanical Engineering, University of Canterbury, Christchurch, New Zealand.

Luciana R. Barroso

Department of Civil Engineering, Texas A&M University, College Station, Texas, USA.

ABSTRACT: Recent research in the area of semi-active control has led to the development of an impressive array of smart dampers and resetable devices. These actuators typically employ control algorithms that are a function of local structural response measurements. However, the structural response of tall structures under seismic loading can have significant contribution from higher modes that can negatively interact with the decentralized nature of the control laws. The interaction of higher modes, non-linear effects and decentralized control on the stability of tall structures is investigated for the SAC-9 steel, moment resisting frame structure. The research is presented in terms of semi-active resetable actuators that use the compressibility of air to create non-linear springs that optimally release stored energy before it is returned to the structure. The action of these devices is governed by local measurements of relative velocity and displacement that can lead to actuator-to-actuator interaction when higher modes are present in the response. These interactions are shown to be a function of non-linear effects and higher mode contributions that result in increased permanent deformations, accelerations and structural hysteretic energy. Highly effective control architectures that mitigate these effects are presented in contrast.

1 INTRODUCTION

In recent years, control systems research has made significant progress in reducing the overall response of civil structures subjected to seismic excitations. Semi-active controllers are the most recent evolution in structural control and offer many of the benefits of active control with power requirements several orders of magnitude smaller eliminating the need for a large external power source. Examples of semi-active controllers include hydraulic actuators and dampers used as energy sinks, where orifice size is the controller parameter (Patten et al, 1994). More recent advances in magneto- and electro-rheological fluids, have led to more advanced systems (Spencer et al, 1996). The objective of the research presented here is to examine the interactions between actuator architecture, semi-active control system performance and the higher mode response of tall structures.

2 DESCRIPTION OF CASE STUDY STRUCTURE

The SAC-9 structure is a 9-story steel moment-resisting frame building (SMRF), denoted SAC9, and designed as part of the SAC steel project for the Los Angeles area. The structural system consists of fixed-base steel perimeter- moment-frames and interior gravity-frames with shear connections. For detailed information on the structural system and its uncontrolled behavior, the reader is referred to the work of Krawinkler and Gupta (1998). Suites of ten different time histories, with two orthogonal directions for each history, were generated for the SAC project to represent ground motions having

probabilities of excedance of 50% in 50 years, 10% in 50 years, and 2% in 50 years in the Los Angeles region, referred to as the 50 in 50 Set, 10 in 50 Set, and 2 in 50 Set with return periods of 72, 474 and 2474 years, respectively (Sommerville et al. 1997). The suites should be used as either a whole set of 20 ground motions or as the 10 different time histories neglecting one orthogonal direction. Note that even the low, 50 in 50 Set of ground motions contains large seismic events given their once in a lifetime probability of occurrence. The acceleration histories have been scaled to conform to the 1997 NEHRP design spectrum for firm soil and the specified return periods.

This study is concerned with response values and demands on the global or story level, for which a lumped plasticity model of the frame elements with centerline dimensions has been selected as appropriate. The frame members are modeled as linear elastic beam-column elements and nonlinear behavior is added by nonlinear torsional spring connections at the ends of the beam-column elements. The model chosen for the nonlinear rotational spring is the Bouc-Wen smooth-varying hysteretic model (Wen 1976; Barroso et al, 2002). To account for P-Δ effects the relationship between compressive axial forces and lateral translations of the column can be written in matrix form as an additional geometric stiffness matrix used to augment the linear elastic stiffness contributions.

3 CONTROL DESIGN AND ARCHITECTURE

Resetable actuators are hydraulic spring elements in which the un-stretched spring length can be reset to obtain maximum energy dissipation from the structural system. With the actuator valve closed energy is stored within the actuator's bi-directional piston-cylinder arrangement, as the actuator is either compressed or extended. At the point when the energy storage rate is stationary the valve between the two cylinder halves is rapidly opened and closed, releasing energy from the system before it is returned to the structure. The attainable range of resetable actuator spring stiffness is extensive. Testing has found that the reset time is approximately 20msecs implying structures with natural frequencies up to about 20 Hz may be effectively controlled (Bobrow et al. 2000).

The control architecture denoted SAC9-A3a has tendons attached between the ground and floors 2 and 3, with an active tuned mass damper (ATMD) placed on the ninth floor. An alternative architecture, denoted SAC9-A3b, has the same configuration but the actuators and tendons are placed on a specific story rather than the ground allowing reaction loads to influence the story. The ATMD is controlled by an independent linear quadratic regulator (LQR) controller focused on top floor displacement, and is employed to ameliorate the top whip of this structure and the loss in lateral actuation force necessitated by a steep tendon angle to that floor. Figure 1 shows these architectures schematically. The total actuator authority for each of the control architectures is 6230kN, which represents 13.6% of the structural weight - a feasible, practical limit. The maximum actuator authority is distributed with 3340, 2000, and 890 kN on the 2^{nd}, 3^{rd}, and 9^{th} floors respectively. The lateral maximum actuator authority on floors 2 and 3 is reduced due to the tendon angle, by factors of 0.89 and 0.81 respectively, for the SAC9-A3a architecture and are much less so for the SAC9-A3b architecture. The primary difference is mounting of the actuators on the individual storys where the reaction loads to actuator forces will impact the structural dynamics, as opposed to the ground mounting in Figure 1 where the reaction forces are effectively nullified.

The control law for each independently controlled, resetable actuator is dependent on the rate of energy storage, with the free length of the hydraulic spring reset when the energy storage is maximised. The energy in a single actuator, U_{act}, is defined:

$$U_{act} = \frac{1}{2} K_{act} (v - v_o)^2 \qquad (1)$$

Where v is the relative displacement of the actuator ends, v_o is the free length of the hydraulic spring set at the last reset position, and K_{act} is the effective spring stiffness. As the idea of the control law is to remove energy from the structural system as quickly as possible, the control law waits until the energy in the hydraulic spring is maximised, thus dissipating maximum packets of energy before re-applying the control force. Discarding maximum packets of energy is advantageous, as it then minimises the actuator valve-open time during which the actuator applies no control force to the structure. Taking

the time derivative of Equation (1), the control logic can be developed by releasing energy when the velocity of the story being controlled changes sign. The control force applied to the structure for a single actuator, u_i, is then simply that of a displaced spring with the additional logic incorporating actuator saturation at level F_{imax}:

$$u_i = \begin{cases} -K_{iact}(v_i - v_{io}) & \text{if } u_i < F_{i\max} \\ -F_{imax}\,\mathrm{sgn}(v_i - v_{io}) & \text{if } u_i > F_{i\max} \end{cases} \qquad (2)$$

It should be noted that the displacement of the ith actuator, v_i, is measured relative to the time-varying dynamic equilibrium point. The inclusion of the structure's permanently deformed position during strong motions reduces the likelihood of the actuator forces allowing the structure to re-yield back to its original static position, which would result in increased structural damage (Hunt, 2002).

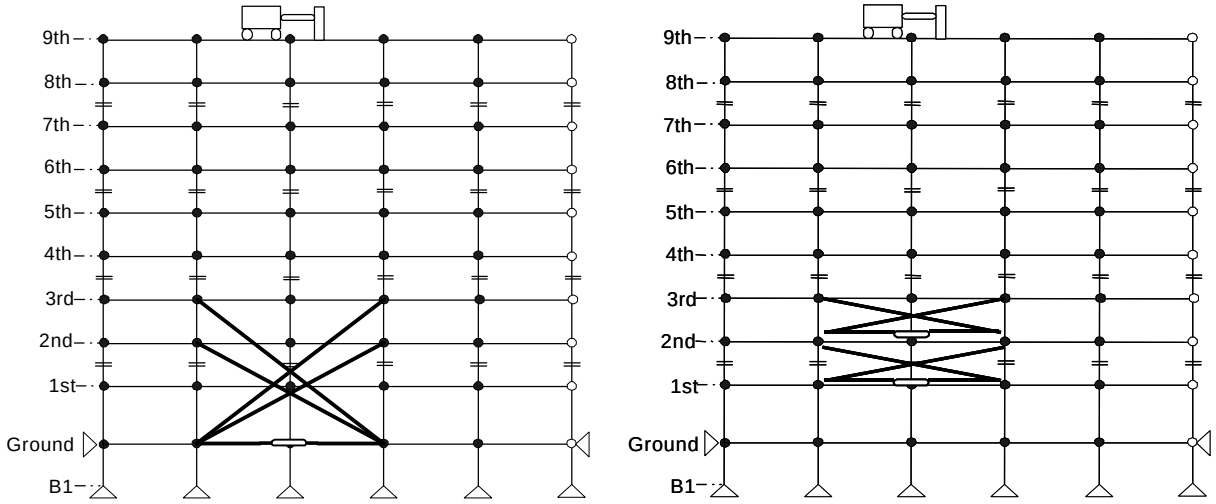

Figure 1: Schematic of SAC9-A3b (left) and SAC9-A3b (right) actuator architectures.

4 SIMULATION AND ANALYSIS

The control architectures in Figure 1 were simulated for the odd half of each suite and statistical response measures were developed for each suite. The primary response statistic of interest is a "best" or central estimate of the peak values that can be statistically quantified over the entire suite of inputs using appropriate lognormal statistics. The metrics employed for this research include peak inter-story drift, peak residual or permanent drift, peak story acceleration and normalized hysteretic energy (NHE). NHE is used to represent cumulative damage while inter-story drift is much more appropriate than the roof drift angle because it can exceed the latter by a factor of two or more (Krawinkler and Gupta 1998). Finally, acceleration demands are of concern for the nonstructural components and occupants of the building. Each of these metrics is quantified using appropriate lognormal statistics for the 50th and 84th percentile levels, which represent the geometric mean and multiplicative variance of the geometric mean respectively. As a result, the sets of ten simulation results are used to quantify the statistical distribution of structural response for seismic events associated with the given input suite's probability of occurrence.

The results for the SAC9-A3a architecture and the high earthquake suite, provided in Table 1, show reductions in peak drift for all floors at each of the three statistical levels, with the exception of the 84th percentile for floor 6, which shows a 1.8% (1.25mm) increase. The geometric mean permanent drifts show reductions at each floor other than floor 3, with an average reduction across all floors of 27.0%. Permanent drifts at the 84th percentile levels show increases at each of the floors, excluding floors 2 and 9, which reduce by more than 10%. This type of reduced geometric mean with increased upper

percentiles represents a stretch of the distribution due to minimal reductions obtained for a few extreme events. Peak accelerations show a general increase across the distribution, with significantly greater increases on floors 2 and 3 where the resetable actuators are applied. The hysteretic energy is reduced on all floors, with average reductions of 52.8% and 42.8% for the 50th and 84th percentiles.

Table 1: SAC9-A3a results for odd-half high suite

	GR	F1	F2	F3	F4	F5	F6	F7	F8	F9
50th percentile										
Peak Drift (%)		-18.47	-24.60	-27.44	-25.34	-22.27	-15.55	-17.82	-21.58	-19.51
Permanent Drift (%)		-30.97	-27.78	7.73	-10.47	-24.13	-70.69	-34.22	-18.20	-33.66
Peak Acceleration (%)		21.82	102.61	50.77	19.33	4.09	12.16	9.24	7.41	17.88
Hysteretic Energy (%)	-74.58	-54.47	-53.80	-35.03	-55.27	-60.47	-37.60	-53.43	-49.51	-54.21
84th Percentile										
Peak Drift (%)		-12.13	-17.17	-19.42	-22.41	-16.29	1.76	-2.41	-7.94	-10.84
Permanent Drift (%)		20.88	-14.03	3.02	21.55	17.81	309.13	97.47	13.99	-21.14
Peak Acceleration (%)		11.46	86.53	26.20	10.15	6.05	11.16	-1.02	-0.38	12.29
Hysteretic Energy (%)	28.11	-39.13	-47.27	-51.66	-58.70	-47.90	-35.58	-53.43	-54.62	-68.20

The response of the SAC9-A3a structure to the medium earthquake suite is better than the high suite, with general reductions in both peak and permanent drifts observed across all levels. As shown in Table 2, average geometric-mean peak and permanent drifts are reduced by 33.5% and 76.6% respectively, while average hysteretic energy is reduced 86.7%. Similar reductions are observed at the higher levels of the distribution, other than for floor 1 permanent drifts, which increase by 168.5% (2.7cm) at the 84th percentile. Although the soft first story adds isolation advantages, a problem is created when the floors directly above it are controlled with decentralised actuator forces, as the soft first story may have very large drifts due to the high stiffness of the controlled floors above, and lack of centralised control design to account for this effect. However, it appears that this first floor drift augmentation only occurs during the extreme events within the suite, with the majority of responses resulting in first floor permanent drift reductions. Peak accelerations are generally increased, with the most significant increases on the actuated floors.

Table 2: SAC9-A3a results for odd-half medium suite.

	GR	F1	F2	F3	F4	F5	F6	F7	F8	F9
50th percentile										
Peak Drift (%)		-14.95	-33.12	-40.90	-38.86	-37.97	-30.17	-32.68	-39.41	-33.25
Permanent Drift (%)		-61.79	-74.81	-70.40	-75.81	-74.78	-80.74	-83.48	-85.06	-82.68
Peak Acceleration (%)		56.05	191.11	104.01	36.91	31.35	20.41	42.26	17.52	17.16
Hysteretic Energy (%)	-24.15	-73.63	-99.82	-98.58	-99.40	-99.93	-99.82	-89.79	-81.81	-99.96
84th Percentile										
Peak Drift (%)		-9.32	-35.30	-43.23	-37.87	-34.26	-30.29	-27.88	-35.01	-37.16
Permanent Drift (%)		168.45	-36.53	-61.10	-78.55	-59.30	-70.40	-43.33	-8.46	-24.19
Peak Acceleration (%)		50.99	147.60	101.55	25.92	30.78	31.89	37.51	0.62	15.98
Hysteretic Energy (%)	-39.21	-73.94	-90.85	-90.40	-88.24	-92.82	-91.81	-82.41	-75.23	-90.72

The results for the low earthquake suite are presented in Table 3 where peak and permanent drifts show significant reductions across all floors and levels. Average geometric-mean peak and permanent drifts are reduced by 55.2% and 92.4% respectively. As with the high and medium suites, peak accelerations show a general increase across the distribution, with the largest increases seen at the second and third floors where actuator tendons are attached. This increase in accelerations appears to be the primary deficiency with the SAC9-A3a,b architecture's combination of decentralised resetable actuators and ATMD architecture attached to floors 2, 3, and 9 only. Hysteretic energy is reduced by an average of 99.7% and 92.8% at the 50^{th} and 84^{th} percentiles respectively, showing the effective energy dissipation ability of the resetable actuator and the SAC9-A3a control architecture.

Table 3: SAC9-A3a Results for odd-half low suite.

	GR	F1	F2	F3	F4	F5	F6	F7	F8	F9
50^{th} percentile										
Peak Drift (%)		-62.41	-61.65	-59.45	-53.82	-53.79	-58.77	-61.82	-47.73	-37.67
Permanent Drift (%)		-98.16	-98.76	-98.79	-98.80	-97.48	-87.49	-84.98	-86.24	-80.43
Peak Acceleration (%)		42.90	145.70	69.52	18.89	3.73	5.81	0.74	-5.83	6.46
Hysteretic Energy (%)	-99.86	-100.00	-100.00	-100.00	-99.97	-99.92	-99.92	-100.00	-99.99	-96.83
84^{th} Percentile										
Peak Drift (%)		-51.82	-49.00	-49.12	-46.01	-43.19	-39.83	-47.75	-37.88	-27.79
Permanent Drift (%)		-98.30	-99.52	-99.66	-99.58	-98.58	-90.26	-93.27	-89.71	-83.76
Peak Acceleration (%)		36.04	89.54	50.85	32.18	-0.13	7.98	2.00	1.35	7.76
Hysteretic Energy (%)	-99.73	-100.00	-99.95	-99.96	-99.99	-99.86	-93.90	-97.74	-89.04	-47.86

The same simulations were also run for the SAC9-A3b architecture of Figure 1. The performance for these cases was marginal compared to the SAC9-A3a case, with increased story drifts and smaller hysteretic energy reductions. Table 4 shows the average geometric mean response (50th percentile) for each of the response metrics and each suite of ground motions. The results clearly show the reduced performance of the SAC9-A3b control architecture, particularly for hysteretic energy and the associated accumulated damage represented by that metric. Peak drifts reductions are significantly lower for each suite although the reductions grow in similar trends. Permanent drifts are actually increased for the high and medium suites and essentially unchanged for the low suite, in contrast to the growing reductions seen with the SAC9-A3a architecture. The tradeoff is that with reduced peak and permanent deflection control the peak story accelerations, particularly for actuated storys, are much lower, representing the accepted compromise between story displacement reduction and increased story acceleration. Note that control architectures with up to 8 actuated storys were trialled and greater numbers of actuators leads to equivalent or greater degradation in control effectiveness.

Table 4: SAC9-A3a and SAC9-A3b Average Geometric Mean Results.

	2 in 50 High Set		10 in 50 Medium Set		50 in 50 Low Set	
	SAC9-A3a	SAC9-A3b	SAC9-A3a	SAC9-A3b	SAC9-A3a	SAC9-A3b
Peak Drift (%)	-21	-3	-34	-8	-55	-15
Permanent Drift (%)	-27	+8	-77	+25	-92	-1
Peak Acceleration (%)	+27	+11	+57	+23	+32	+25
Hysteretic Energy (%)	-53	-12	-87	-36	-99	-56

With the potential of resetable actuators identified using a three-story structure (Barroso et al, 2002), it was recognised that the different, and potentially multi-mode, response characteristics of the SAC9 structure may have a significant impact on control performance. The residual permanently deformed shape of the uncontrolled structure gives an indication of the predominant modes of the dynamic response, as well as the shape around which the structure oscillates after the initial strong motion. The deformed shape shown in Figure 2b represents the final equilibrium position about which the structure oscillates. Figure 2b shows the relative permanent story drifts, which clearly reduce above floor 3. If the response were solely first mode, one would expect the permanent drifts to be approximately constant, which is not the case.

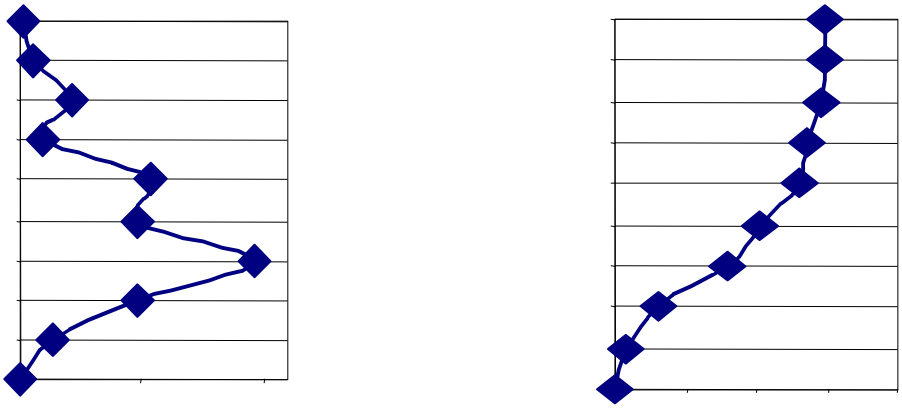

(a) (b)

Figure 2: SAC9 uncontrolled yielded response. (a) Permanent drifts. (b) Permanently deformed shape.

Although the modal contributions shown in Table 5 are predominantly first mode, the contributions of the 2nd and particularly 3rd and 4th modes are significant. The influence of higher modes is the primary difference between the SAC3 and SAC9 structural responses, and requires adjustment of how the control laws are designed and implemented for the SAC9 and other taller, multi-mode response structures. Note that with a linear simulation the modal contributions are over 95% first mode and as a result the interaction of other modes in the response is minimal to none, illustrating the necessity of non-linear modelling for control system development.

Table 5: Modal contributions to SAC9 uncontrolled permanently deformed shape – Kobe Earthquake.

Mode	Contribution to Deformed Shape (%)
1	74.6
2	1.8
3	-7.7
4	6.1
5	-2.8
6	2.5
7	-0.3
8	-1.4
9	-2.8

When higher modes are present, actuators placed on adjacent or moving storys may have a negative effect due to the equal and opposite reaction forces applied to the floors on which they are placed. For the resetable actuator, with higher modes present the velocity of the floors may be slightly out of

phase. Hence, the decentralised controller may apply forces for which the reaction forces augment the response of some floors while attempting to restrict others. This effect is shown schematically in Figure 3, where forces F_1 and F_3 are acting to restore floors 2 and 3 back to the equilibrium position based on the relative velocities and displacements employed. However, the combination of these forces, F_2, is tending to push the second floor away from the equilibrium position. This interaction can easily occur if higher modes cause the relative velocity of floor 1 and 2 to be less than or near zero, or if their displacements are nearly equal as shown in the figure. Similar actuator-actuator interactions are expected using centralised control design methods such as LQR, as the oscillation about the higher mode deformed shape is not accounted for by linear control design methods, and the higher mode contributions are therefore much smaller. In addition, with actuators on each floor reaction loads can, at best, cancel out the effect of the actuator below, and, at worst, accelerate certain floors away from their equilibrium position causing greater damage.

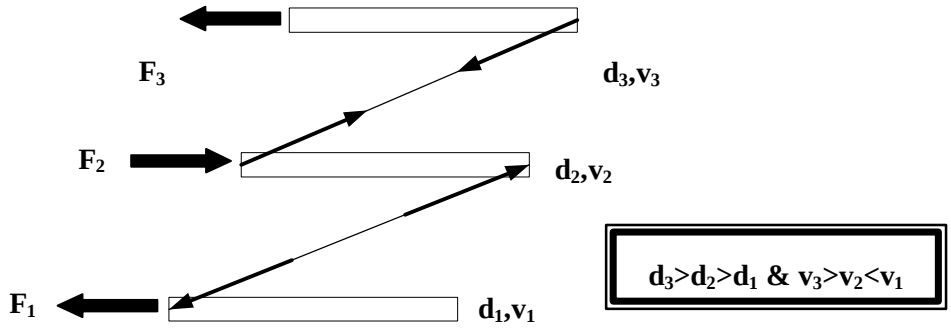

Figure 3: Schematic of actuator-actuator interaction for resetable controller.

Hence, for the SAC9 and other taller structures, actuators should probably not be placed between individual floors due to this coupling of actuator forces through higher mode contributions that can lead to augmented response. Instead, actuator authority can be applied via tendons between the ground and the respective upper floors. This approach is more effective as it removes the possibility of this type of actuator-actuator interaction.

5 CONCLUSIONS

The interaction of decentralised control algorithms for semi-active control, such as the use of resetable actuators, and the multi-mode response of tall structures has been demonstrated using the SAC9 steel moment resisting frame. The reaction loads from resetable actuators on a given story has been shown to cause the control performance to degrade significantly compared to similar control architectures where the reaction loads have been nullified by connection to the ground. The use of non-linear structural models that include permanent deformation, rather than linear systems, has been shown to be a primary cause of larger concentrations of higher modes in the structural response that in turn can lead to the actuator-actuator interaction that reduces control efficacy. Similar results may be expected when centralised controllers are used while the use of greater numbers of actuators in the control architecture will exacerbate the effect.

6 ACKNOWLEDGEMENTS

The authors would like to acknowledge the New Zealand Earthquake Commission EQC Research Fund, Grant #01/U482, for their support of this research.

REFERENCES

Barroso, L., Chase, J. Geoffrey and Hunt, S. (2002). "Smart-Dampers for Multi-Level Seismic Hazard Mitigation of Steel Moment Frames," Proc. of the 3rd World Conf on Structural Control (3WCSC), Como, Italy, April 7-12.

Bobrow, J.E., Jabbari, F., Thai, K. (2000). "A new approach to shock isolation and vibration suppression using a resetable actuator," *ASME Trans. on Dynamic Systems, Measurement and Control* , vol 122, pp. 570-573.

Hunt, S., Chase, J. G. and Barroso, L. R. (2002). "The Impact of Time Varying Equilibrium Location in the Semi-Active Control of Non-Linear Seismically Excited Structures," Proc. of ICARCV 2002, Singapore, Dec 3-5 (in press).

Krawinkler, H., and Gupta, A. (1998). "Story Drift Demands for Steel Moment Frame Structures in Different Seismic Regions." 6th National Conference on Earthquake Engineering, Seattle, WA.

Patten, W. N., He, Q., Kuo, C. C., Liu, L. and Sack, R. L. (1994). "Suppression of Vehicle Induced Bridge Vibration Via Hydraulic Semi-Active Actuators," Proc. 1st World Conf on Struct. Control, FA1, 3-38.

Sommerville, P., Smith, N., Punyamurthula, S., and Sun, J. (1997). "Development of Ground Motion Time Histories for Phase II of the FEMA/SAC Steel Project." SAC Background Document Report No. SAC/BD-97/04.

Spencer, B. F., Dyke, S. J. and Sain, M. K. (1996). "Magnetorheological Dampers: a new approach to seismic protection of structures," Proc. Conf on Decision and Control, pp. 676-681.

Wen, Y. K. (1976). "Method for Random Vibration of Hysteretic Systems." Journal of Engineering Mechanics Division, 102(EM2), 249-263.